remote sensing

MDPI

Article

A Comparative Crash-Test of Manual and Semi-Automated Methods for Detecting Complex Submarine Morphologies

Vasiliki Lioupa [1], Panagiotis Karsiotis [1], Riccardo Arosio [2], Thomas Hasiotis [1,*] and Andrew J. Wheeler [2,3]

[1] Department of Marine Sciences, University of the Aegean, 81100 Mytilene, Greece; mard20010@marine.aegean.gr (V.L.); marm623003@marine.aegean.gr (P.K.)
[2] School of Biological, Earth and Environmental Sciences, Environmental Research Institute, University College Cork, Distillery Fields, North Mall, T23 TK30 Cork, Ireland; rarosio@ucc.ie (R.A.); a.wheeler@ucc.ie (A.J.W.)
[3] SFI Research Centre in Applied Geosciences (iCRAG), SFI Research Centre for Energy, Climate & Marine (MaREI), University College Cork, T23 TK30 Cork, Ireland
* Correspondence: hasiotis@aegean.gr

Abstract: Multibeam echosounders provide ideal data for the semi-automated seabed feature extraction and accurate morphometric measurements. In this study, bathymetric and raw backscatter data were initially used to manually delimit the reef morphologies found in an insular semi-enclosed gulf in the northern Aegean Sea (Gera Gulf, Lesvos Island, Greece). The complexity of this environment makes it an ideal area to "crash test" (test to the limit) and compare the results of the delineation methods. A large number of (more than 7000) small but prominent reefs were detected, which made manual mapping extremely time-consuming. Three semi-automated tools were also employed to map the reefs: the Benthic Terrain Modeler (BTM), Confined Morphologies Mapping (CoMMa), and eCognition Multiresolution Segmentation. BTM did not function properly with irregular reef footprints, but by modifying both the bathymetry and slope, the outcome was improved, producing accurate results that appeared to exceed the accuracy of manual mapping. CoMMa, a new GIS morphometric toolbox, was a "one-stop shop" that, besides generating satisfactory reef delineation results (i.e., detecting the same total reef area as the manual method), was also used to extract the morphometric characteristics of the polygons resulting from all the methods. Lastly, the Multiresolution Segmentation also gave satisfactory results with the highest precision. To compare the final maps with the distribution of the reefs, mapcurves were created to estimate the goodness-of-fit (GOF) with the Precision, Recall, and F1 Scores producing values higher than 0.78, suggesting a good detection accuracy for the semi-automated methods. The analysis reveals that the semi-automated methods provided more efficient results in comparison with the time-consuming manual mapping. Overall, for this case study, the modification of the bathymetry and slope enabled the results' accuracy to be further enhanced. This study asserts that the use of semi-automated mapping is an effective method for delineating the geomorphometry of intricate relief and serves as a powerful tool for habitat mapping and decision-making.

Keywords: multibeam echosounder; geomorphology; benthic terrain modeler; reef mapping; semi-automatic delineation; CoMMa; eCognition

check for updates

Citation: Lioupa, V.; Karsiotis, P.; Arosio, R.; Hasiotis, T.; Wheeler, A.J. A Comparative Crash-Test of Manual and Semi-Automated Methods for Detecting Complex Submarine Morphologies. *Remote Sens.* **2024**, *16*, 4093. https://doi.org/10.3390/rs16214093

Academic Editors: Alessandra Savini, Luca Fallati and Gema Casal

Received: 29 August 2024
Revised: 18 October 2024
Accepted: 31 October 2024
Published: 2 November 2024

Copyright: © 2024 by the authors. Licensee MDPI, Basel, Switzerland. This article is an open access article distributed under the terms and conditions of the Creative Commons Attribution (CC BY) license (https://creativecommons.org/licenses/by/4.0/).

1. Introduction

The geomorphometry of seafloor terrain is a common study that can be applied to multibeam echosounder (MBES) data to categorize, visualize, and quantify the seabed based on its abiotic characteristics, which can also assist in benthic habitat appraisals [1]. The outputs are of relevance in decision-making, spatial planning, and ecological management by governmental and environmental organizations [2].

The simplest method is manual mapping: the expert uses bathymetric and backscatter data to determine the final zone boundaries on the map. Until recently, this method

was considered to be the most reliable [3], although time-consuming. Still, many semi-automated methods that have been used for geomorphometry and/or benthic habitat mapping show promising results, although they also have their challenges [4]. Many different approaches have been tried to date but there is not a unified protocol as each case study is different, and the main focus of each survey may require several modifications to the method [5].

One of these methods is the Benthic Terrain Modeler (BTM), which was developed in 2005 at Oregon State University in collaboration with the NOAA Coastal Services Center (CSC) GIS Integration and Development program [6,7]. This geoprocessing toolbox analyses benthic terrain and produces bathymetric derivatives, such as slope, aspect, and Bathymetric Position Index (BPI), a variation on the Topographic Position Index [8,9]. The tool is a free add-on in ArcGIS and it is widely used. Some recent studies have used the BTM toolbox to support spatial management [10], habitat mapping [11–14], sediment distribution [15], paleogeomorphology [16,17], human impacts and geohazards [18], predictive habitat distribution models [19–21], and deriving spatial patterns for hydrodynamic processes [22]. In most of the above-mentioned studies, the underwater relief was relatively even, except in cases of submarine canyons where BTM was successfully used [23,24]. The accuracy of BTM has never been fully analyzed.

A new tool, the Confined Morphologies Mapping (CoMMa) Toolbox, was developed as an add-on for ArcGIS Pro. With this toolbox, originally created for multibeam data, the user can use the Data Preparation tools to compensate for data artefacts and create Local Topographic Position (LTP) derivatives, use the Delineation tools to map terrain features, and finally use the Description tools to calculate the geomorphological characteristics of the delineated features. The results can be used to understand spatial patterns in the shape, biodiversity, and environmental conditions (e.g., current speeds and direction) of seabed features, such as cold-water coral mounds [25].

Lastly, eCognition is an object-based analysis software from Trimble that was developed originally for satellite image analysis [26]. This tool has been applied to MBES data for the habitat mapping of various features in marine environments [22,26,27] and has been proven to produce good results.

In this study, the unique geomorphology of a semi-enclosed embayment (Gera Gulf) on Lesvos Island (NE Aegean Sea, Greece) (Figure 1) was the test site for the semi-automated delineation methods. Manoutsoglou et al., (2018) [28] described a large number of low-relief buildups using information single-beam echosounder profiles and a side-scan sonar mosaic. Ground-truthing using drop-camera, scuba dives, and sampling verified the presence of numerous small reefs consisting of benthic assemblages dominated by molluscs in a fine-grained environment. They suggested that 19.27 km^2 of the surveyed area is occupied by about 4400 densely distributed reefs, which are 0.2–2.5 m in height. In this study, high-resolution MBES data from the gulf revealed more than 7000 small reefs with complex morphologies, some discrete and others merged. Mapping their morphological characteristics could provide more information about their formation and growth mechanisms. This rich and complex terrain provided a perfect natural laboratory to "crash test" (determine the performance limits of) the manual and semi-automated methods. As such, the high-resolution MBES data are used here to: (i) compare the results of the manual mapping of the complex relief of the gulf seafloor with three semi-automated methods (BTM, CoMMa, and eCognition); (ii) enhance the MBES bathymetry in order to assist BTM to better detect the reefs; and (iii) assess the suitability of these semi-automated methods for complex low-relief reef mapping, comparing the resulting maps with the goodness-of-fit index, a method that compares the overlap of polygons [29].

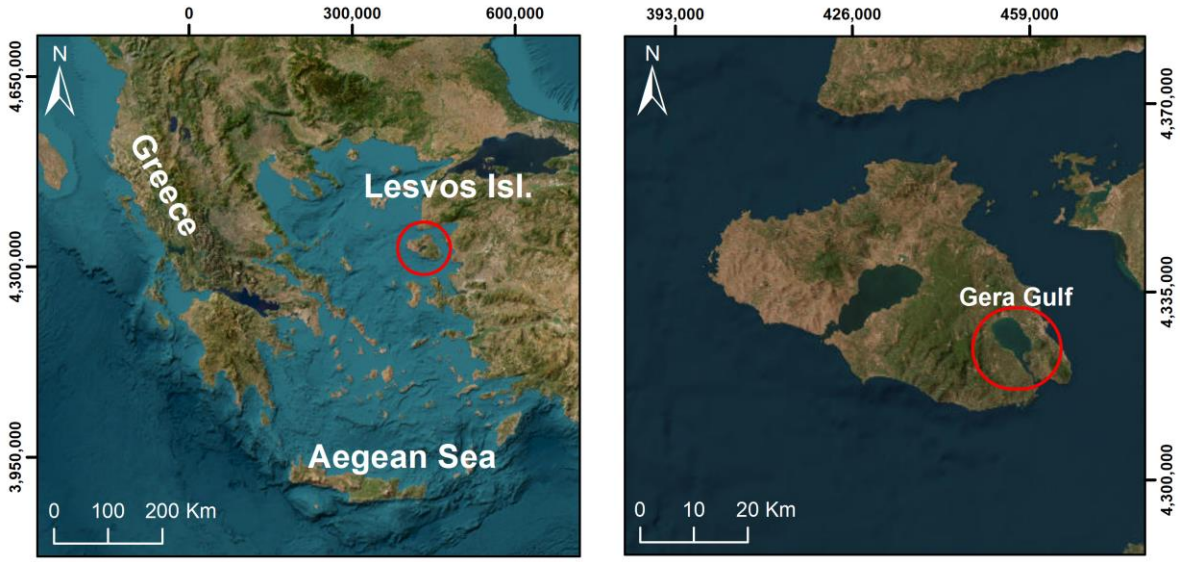


Figure 1. The location of the study areas (Gera Gulf) in Greece and Lesvos Island (red circle).

2. Materials and Methods

2.1. Data Acquisition and Processing

Bathymetric surveys took place in April and November 2022 using the Teledyne Reson SeaBat T20-R MBES (Teledyne Marine, Slangerup, Denmark), pole-mounted in R/V Amfitriti. The MBES comprised a TC2181 transducer, an EM7219 receiver, a Valeport mini SVS for the correct swath projection, and a rack-mounted sonar processor, which is configured with a fully integrated inertial navigation system (INS), Teledyne, Type-20. The INS uses an IMU (IP68) for motion correction (roll, heave, and acceleration measurements) and a RTK GNSS (Trimble, Westminster, CO, USA) for position, time, and high-precision navigation. The INS is fully compliant with the Applanix POS MV Wavemaster II (Applanix Corporation, Richmond Hill, ON, Canada) integrated into a T20R processor. The vessel's speed ranged from 3 to 4 knots. An area of about 30 km^2 was surveyed (~75% of the total gulf area). The system simultaneously recorded 512 beams at 420 kHz over a swath angle of up to 140°. Sound velocity profiles were collected using a Valeport SWiFT. The bathymetric data were calibrated, sound velocity profiles were applied, and any acoustic noise or artifacts were removed utilizing the Teledyne PDS software v. 4.4.4.3. A bathymetric ASCII file with 1-m cell size was exported from the PDS. The raw backscatter data were also exported with a 1-m cell size. The coordinate system of the collected data is WGS84 UTM 35N.

2.2. Manual Mapping

For the manual mapping of the reefs, the bathymetry ASCII file was imported into ArcMap v. 10.4. The *Spatial Analyst Tool* was used to generate the slope and curvature layers. The users employed bathymetry, slope, curvature, and backscatter to manually map the reefs. In the shallower areas, the reefs had a smaller relief, and their shape became more complex making it harder for the users to map their boundaries. In these areas, the users drew profiles on the bathymetric map to make the correct decision, whilst in some cases, changing the contrast of the view was also effective. The shapefile that was created from the manual mapping was used to extract the bathymetry for each of the polygons with the Spatial Analyst tool, Extract by Mask. Next, the geomorphometry characteristics (maximum, minimum, and average depth; maximum and minimum slope; area; perimeter; depth standard deviation; and slope standard deviation) were extracted and matched to the polygon shapefile using Join. The Statistics tool was used to extract the statistical information about the geomorphometry of the reefs.

2.3. Semi-Automated Mapping

For the semi-automated mapping, three methods/tools were used: the Benthic Terrain Modeler toolbox v. 3.0 [30], Confined Morphologies Mapping (CoMMa) Toolbox v. 1.2 [24], and eCognition v. 1.3.

2.3.1. BTM and Bathymetric Enhancement

Initially, reef detection with BTM was not satisfactory (for this trial, the same BPI radius and classification dictionary as described later for B4 and B4S2 were used), since only 50.3% of the reefs were detected that occupied an area about 90% smaller than that occupied by the manually mapped reefs. Furthermore, some BTM mapped reefs were also found to have considerable differences in their shape and geomorphometric characteristics. Therefore, the Raster Calculator was used to enhance the bathymetry and slope, by essentially creating two new "relief-enhancing" derivatives to better discriminate and isolate the small reefs in this peculiar seafloor terrain. Two attempts were tested, the first using only bathymetry and the second using the bathymetry and slope combined, respectively named BTM-B4 and BTM-B4S2.

BTM-B4

The first relief-enhancing derivative (B4) was created using the following expression: z^4, where z is the value of a pixel in the bathymetry raster.

With this modification, the separation of the depth values between adjacent pixels was increased, resulting in the discretization of the reefs. Then, the standard BTM workflow was followed, creating broad (inner radius: 10, outer radius: 100) and fine (inner radius: 10, outer radius: 25) Bathymetric Position Index (BPI) factors that were found to work best for the study area after various trials. The classification dictionary (Table 1) was edited according to the study area and the features to be delineated. As the reefs were detected in water depths deeper than 10 m, a boundary was placed along the 10-m isobath in the classification dictionary to avoid redundant artifacts.

Table 1. Classification dictionary used for creating the BTM reefs.

Method	Class	Zone	Broad BPI Lower	Broad BPI Upper	Fine BPI Lower	Fine BPI Upper	Slope Lower	Slope Upper	Depth Upper
BTM-B4	1	reef	−2000	1	−6000	0	0	15.08	12.5
	2	other	1	2000	−20	6000	0	68	10
BTM-B4S2 reef slope	1	reef	−20,000	2	−20,000	0	0.001	15.08	10
	2	other	2	20,000	0	20,000	0	68	10
BTM-B4S2 reef peak	1	reef	−2000	5	−6000	0	0	15.08	12.5
	2	other	1	2000	0	6000	0	68	10

In order to eliminate the artifacts generated using the semi-automated method created in areas of successive MBES swath overlap, polygons with an area of less than 8 m^2 and a height of less than 5 cm (the maximum extent of the observed false polygons in areas of overlapping bathymetry) were deleted. This step was repeated for all the methods (manual, BTM, CoMMa, and eCognition). Finally, Eliminate Polygon Parts was used to fill in any gaps in some small polygons, Smooth Polygon to smooth the polygons with the PEAK algorithm and a smoothing tolerance of 10, Buffer to create a small buffer of 0.1 m around the reefs, and then *Dissolve* to merge any overlapping polygons.

BTM-B4S2

The second bathymetry-enhancing derivative (S2) was created using the following expression: $(z - slope^2) \times 100$, where z is the depth value of a pixel and "slope" is the slope value as calculated using the ArcGIS tool. This modification places more emphasis on

the variation of the slope of the reefs rather than on the overall bathymetry of the terrain, making it easier for both the user and the BTM to detect the reefs.

This calculation produces a good outline of the reefs but leaves the centers with lower values. Therefore, the "B4" derivative was merged with "S2", leading to positive values for the entirety of the reef forms (B4S2). Broad and fine BPIs were created for both the S2 and B4S2 derivatives, with the same neighborhood size used for the B4 derivative and a modified classification dictionary as shown in Table 1.

For a final "touch-up", Eliminate Polygon Parts was used to fill in any gaps in some small polygons, Smooth Polygon to smooth the polygons, and Buffer to create a small buffer of 0.1 m around the reefs, in order to use the Dissolve tool to merge any overlapping polygons. The following procedures are the same as those outlined in the manual technique to determine the geomorphology.

2.3.2. CoMMa

This toolbox includes three toolsets that allow the user to pre-process multibeam data and calculate local topographic parameters (parameters that are essentially mathematical derivations of DEMs, for example, slope, surface curvature, topographic position, etc.), delineate potential features, and describe the morphological characteristics of confined features (basic, texture, and volume descriptor tools). In order to calculate the basic geometrical and statistical attributes for each reef contained in the delineation shapefile, Comma's Basic Descriptors Tool was used. The resulting attribute table of this tool contains some of the following fields: area, mean reef perimeter (m), max reef area (m^2), sum. Area (km^2), max. height (m), mean height (m), and mean Polsby–Popper circularity test (a measure of the feature compactness) [25,31].

After testing different variables and neighborhood sizes, the Local Topographic Potion (LTP) derivatives tool was used to create a raster with the minimum median filter (setting: inner radius = 5, outer radius = 30) as the best fit for the study area. Then, the Boundary-based Delineation tool was used to map the positive features only and delete internal holes, with DEM (the bathymetry), LTP (the raster created in the previous step), vertical cutoff (=0.1), minimum vertical threshold (=0.1), minimum width (=0), minimum width/length ratio (=0), and buffer (=2). This resulted in a reef delineation shapefile, which was inserted in the Basic Descriptors tool to calculate the morphometric characteristics of all the reefs. The Volume tool was used for the reefs produced using manual mapping, to calculate their volume.

2.3.3. eCognition

This software utilizes advanced algorithms for image segmentation, classification, and change detection, enabling users to perform a detailed analysis of the spatial data [26]. In eCognition, the Multi Resolution Segmentation algorithm was used for reef segmentation (with the settings: parameter = 1, the LTP raster = 2, slope (scale = 5), shape = 0.1, compactness = 0.1, class $\geq$ 0.19). This algorithm employs an optimization procedure that minimizes the average heterogeneity of the image objects at a specific resolution. The scale parameter is an abstract concept that sets the maximum allowable heterogeneity for the resulting image objects [26]. The polygons segmented were inserted in ArcGIS Pro where Smooth Polygon corrected the pixelized edges and CoMMa's Basic Descriptors tool calculated their morphometric characteristics.

2.4. Statistical Comparison

2.4.1. Polygon Overlap Comparison

Mapcurves, a quantitative goodness-of-fit (GOF) method [29], was chosen for the map (manual, BTM-B4, BTM-B4S2, CoMMa, eCognition) overlap comparison and an ArcGIS Pro toolbox was created to automate this calculation (see Supplementary Material for the script). The method presents the degree of spatial concordance between two or more maps and it is based on the degree of spatial overlap between the maps. The reference map

(RF or Map 1) to which another map (Map 2) is compared determines the direction of the comparison, and the combination that produces the best degree-of-fit value is considered to be the level of similarity between the maps. The GOF algorithm (Equation (1)) is based on two values (Figure 2): (1) the proportion of the intersecting area (C) to the total area of the intersecting category from Map 2 (B + C); and (2) the proportion of the intersecting area (C) to the total area of the category from Map 1 (A + C). The first term gives the proportion of "insideness" that the reference category shares with the tested category, and itself represents a GOF term. The second term weights this degree-of-fit by the fractional share of the Map 1 category's area that is intersected. Without that area weighting, the presence of many large intersecting categories, each one of which might share only a small spatial intersection with the category being tested, would result in a high degree of fit. Multiplying these two values, a single number for the total percentage of overlap for the reefs in each map arises. All the possible combinations were tested in order to determine the optimum one.

$$Goodness - Of - Fit = \sum \left(\frac{C}{B + C} \right) \times \left(\frac{C}{A + C} \right) \quad (1)$$

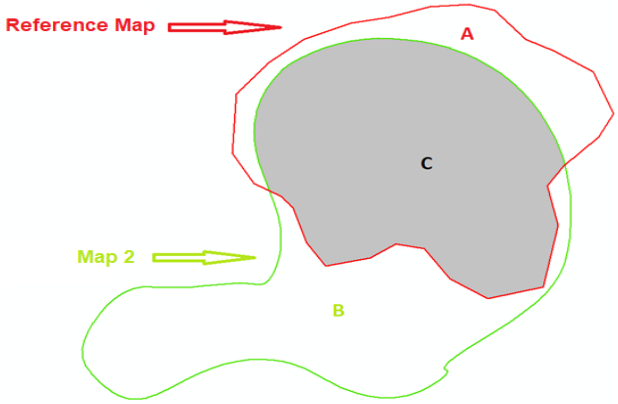


Figure 2. Sketch of overlapping maps (reefs) representing the values of GOF (A: reef area of the reference map, B: reef area of the second map, and C: overlapping area between reef A and B).

Intersect was used to merge each polygon pair, Calculate Geometry to calculate the polygon area, and finally Spatial Join. Using the Join command and the FID as a criterion, the attribute tables of the polygons were matched. The FID and area values of the attribute table were exported into an Excel file, where the GOF values were calculated (Figure 3). Then, the percentage of polygons that satisfied a series of increasing values (every 0.01) of the GOF index (COUNTIF command) was calculated and the according mapcurve graph was created. Mapcurve is a GOF power curve showing the decline in the percentage of map categories in the *y*-axis that still satisfies an increasing GOF threshold on the *x*-axis. The area under the curve of the graph was calculated, providing a unique GOF value for the entire map.

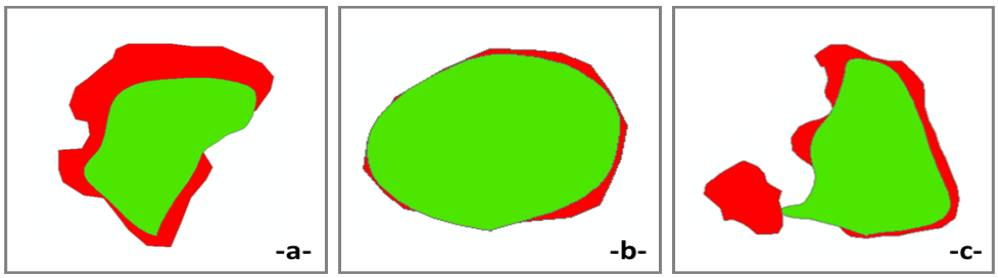


Figure 3. Sketch showing polygons with (**a**) unique, (**b**) maximum, and (**c**) low GOF values (red polygon: manual mapping, green polygon: BTM-B4).

2.4.2. Detection Accuracy

For the polygons that were not detected using the semi-automated or manual methods and vice versa, Precision, Recall, and F1 Score statistical indexes were calculated. Precision is the quotient of the successfully detected reefs with the total number of reefs detected from the method tested. Recall is the quotient of the successfully detected reefs with the total number of reefs detected from the reference method. The F1 Score (Equation (2)) is a weighted average of Precision and Recall, taking values from 0 to 1 (1 corresponds to the highest precision).

$$F1 = 2 \times \frac{Precision \times Recall}{Precision + Recall} \quad (2)$$

For calculating these indexes, manual mapping was considered as the reference method.

2.4.3. Correlation of Geomorphological Characteristics

Using Excel v. 2409, scatter plots of the various geomorphological characteristics were created, trend lines were plotted, and using regression from the data analysis, R^2 and *p*-value were calculated to detect if there were correlations between the geomorphological characteristics of the reefs and the depths they are located in. The scatter plots that were generated were depth/height, slope/depth, area/depth, maximum slope/height, and area/height.

3. Results

The bathymetry of the inner Gera Gulf gradually deepens toward the center, reaching about a 19-m water depth, and connects with the Aegean Sea through a narrow channel (Figure 4). Irregular small topographic features (reefs) are bathymetrically expressed throughout the gulf below a 10-m water depth (Figures 4 and 5).

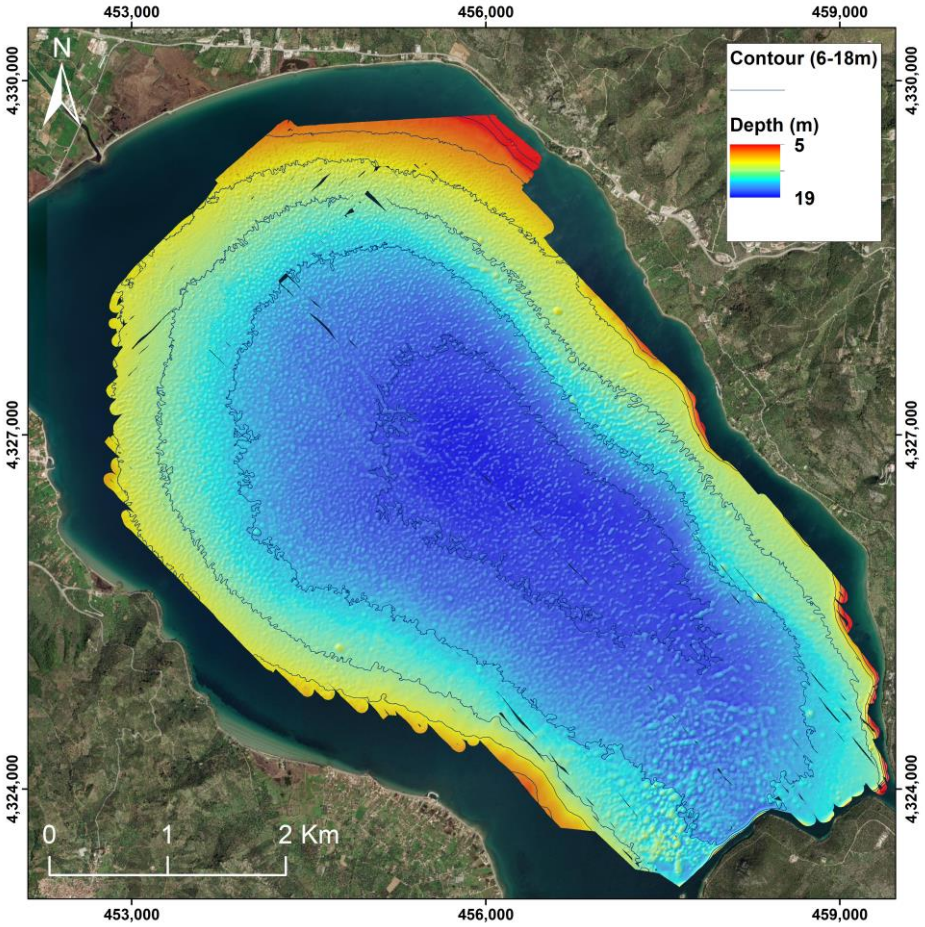


Figure 4. Bathymetric map of the inner Gera Gulf with 2-m interval contours for a depth of 6 to 18 m.

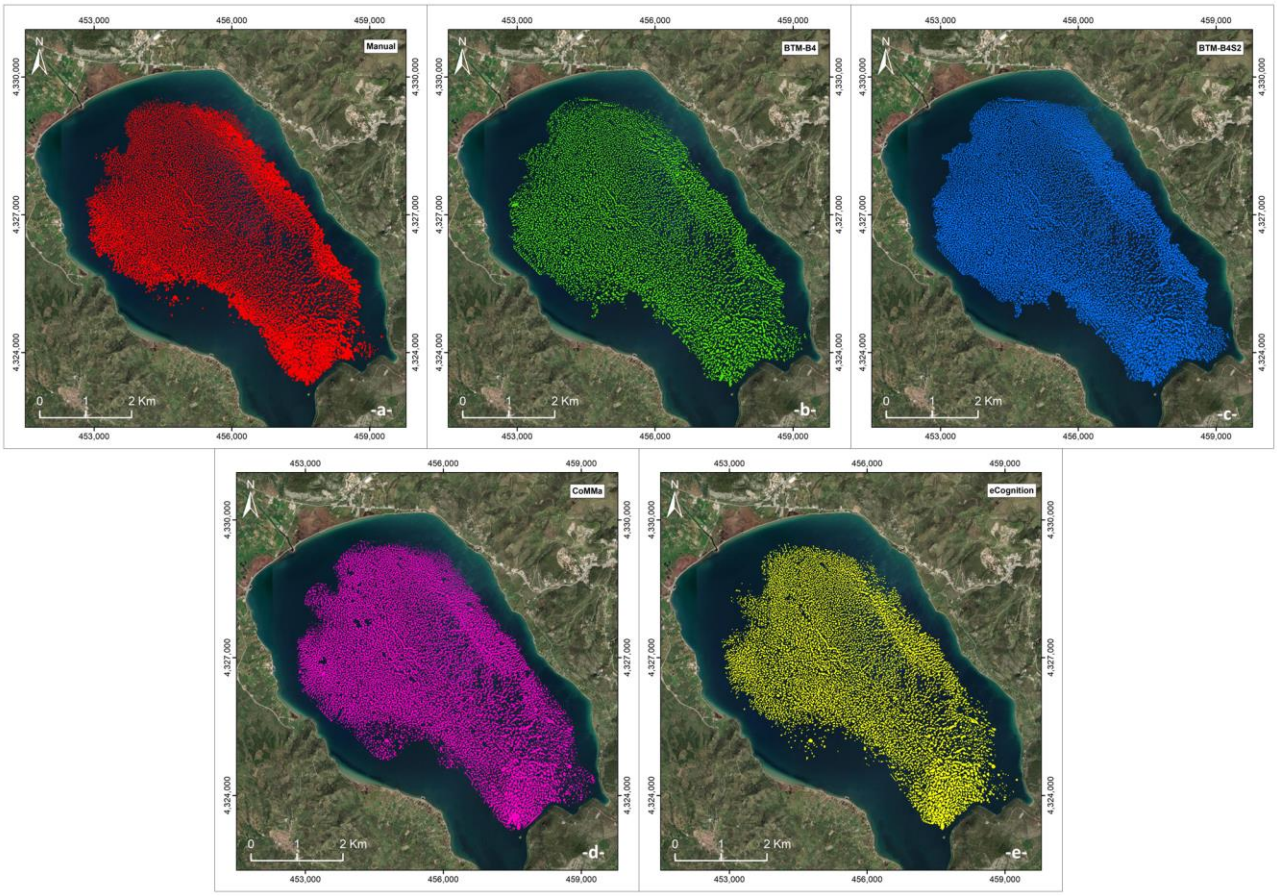


Figure 5. Polygons (reefs) produced using (**a**) manual, (**b**) BTM-B4, (**c**) BTM-B4S2 mapping, (**d**) CoMMa mapping, and (**e**) eCognition mapping.

Overall, 7115 reefs were manually detected, occupying an area of 10.4 km^2 (Table 2). Compared with the number of reefs mapped by Manoutsoglou et al., 2018, this study exceeded it by approximately 3000 more reefs. The four methods used for the Gera Gulf reef detection resulted in four polygon shapefiles (Figure 5) and for each one, the geomorphological features were extracted (Table 2). An example of the overlapping polygons in four different areas in the gulf is shown in Figure 6. The reefs detected using BTM-B4 were 7441, using BTM-B4S2 were 8923, using CoMMa were 7680, and using eCognition were 5649. Both statistics as well as a visual assessment were used to estimate the quality of the results.

Table 2. The geomorphometry results of manual, BTM, BTM-B4, and BTM-B4S2 mapping.

Method	Number of Reefs	Mean Reef Perimeter (m)	Max Reef Area (m^2)	Sum. Area (km^2)	Max. Height (m)	Mean Height (m)	Mean Polsby–Popper Circularity Test
Manual	7115	147	215,743	10.4	4.5	0.65	0.75
BTM	3576	60	7899	1.1	3.0	0.25	-
BTM-B4	7441	120	35,478	6.8	2.7	0.47	0.77
BTM-B4S2	8923	142	147,497	10.3	3.7	0.54	0.68
CoMMa	7680	138	86,308	10.4	3.9	0.56	0.82
eCognition	5649	153	125,905	7.5	4.3	0.71	0.76

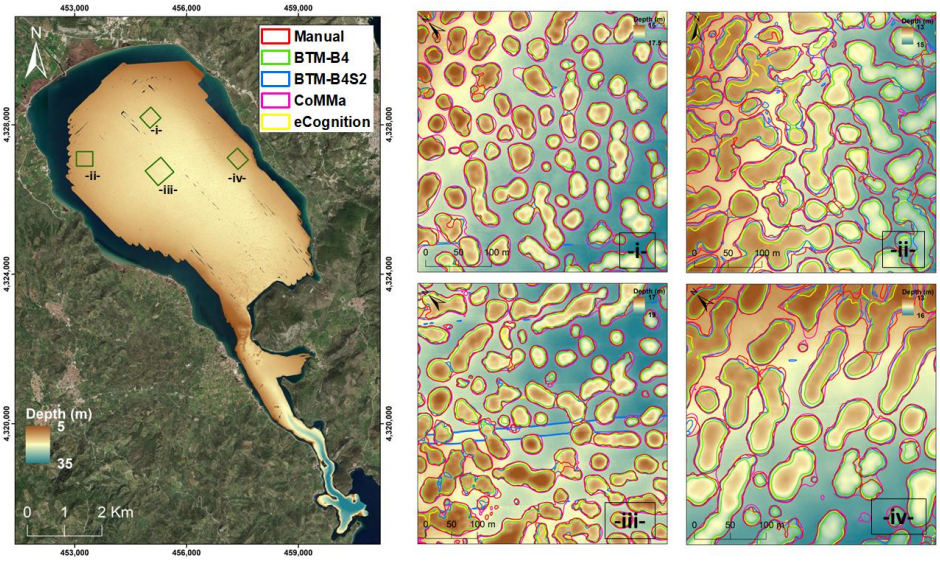


Figure 6. Bathymetric map of the Gera Gulf, with zoom-in areas (**i**–**iv**) showing the resulting polygons for all the methods (red polygons: manual, green: BTM-B4, blue: BTM-B4S2, magenta: CoMMa, yellow: eCognition).

In areas where the relief is complex, manual mapping considered that the reefs were united, whilst most semi-automated methods tended to fragment these large reefs into smaller polygons, thus resulting in more reefs. Consequently, manual mapping produced polygons with very large areas, perimeters, and heights, reaching 0.26 km^2 and 4.5 m respectively, near the gulf entrance, contrasting with the semi-automated methods' polygons. The results of the area and height distribution were visualized into the same categories for all methods used (Figures 7 and 8). It appears that the geomorphology detected using the BTM-B4S2 and CoMMa methods was closer to the results of the manual mapping (Table 2). The biggest difference in the number of reefs between the manual and the semi-automated methods resulted from BTM-B4S2 and eCognition because these methods tended to fragment the polygons the most. The total area of the reefs is the same between the manual and CoMMa methods and it differs by just 0.01 between the manual mapping and BTM-B4S2. The volume of the reefs calculated for manual mapping using the CoMMa toolbox was 2,525,314 m^3.

The polygons detected using manual mapping were also compared with those not detected using the semi-automated methods and vice versa (Figure 9 and Table 3). Manual mapping failed to detect 567 reefs distinguished using BTM-B4, 1939 reefs detected using BTM-B4S2, 1498 reefs detected using CoMMa, and 97 reefs detected using eCognition, most of which are in the shallower part where complex morphology is observed. As for the semi-automated methods, BTM-B4 failed to detect 993 reefs, BTM-B4S2 failed to detect 236 reefs, CoMMa failed to detect 477 reefs, and eCognition failed to detect 1646 reefs distinguished using manual mapping. These reefs are small in height and area.

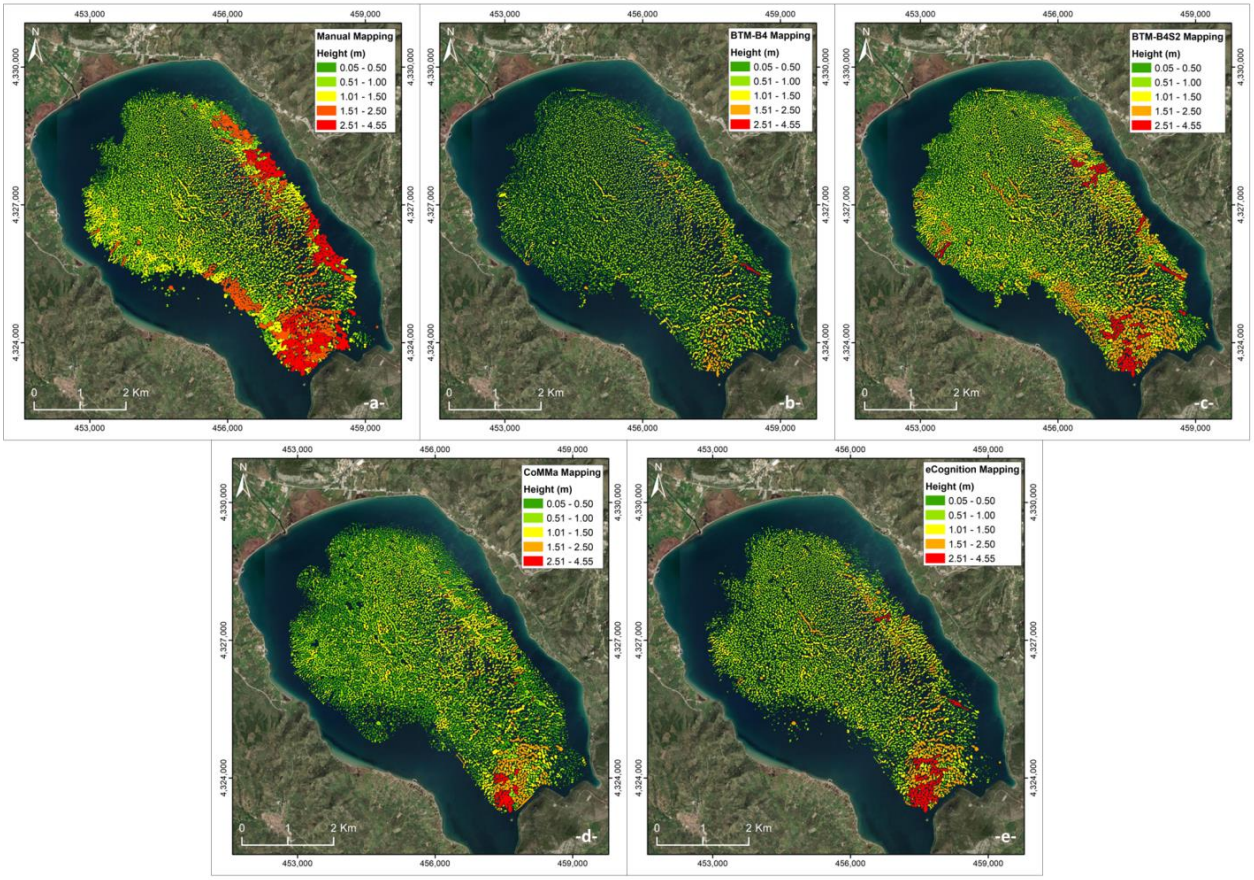


Figure 7. Categorization of the reef heights, created using (**a**) manual, (**b**) BTM-B4, (**c**) BTM-B4S2 mapping, (**d**) CoMMa mapping, and (**e**) eCognition mapping.

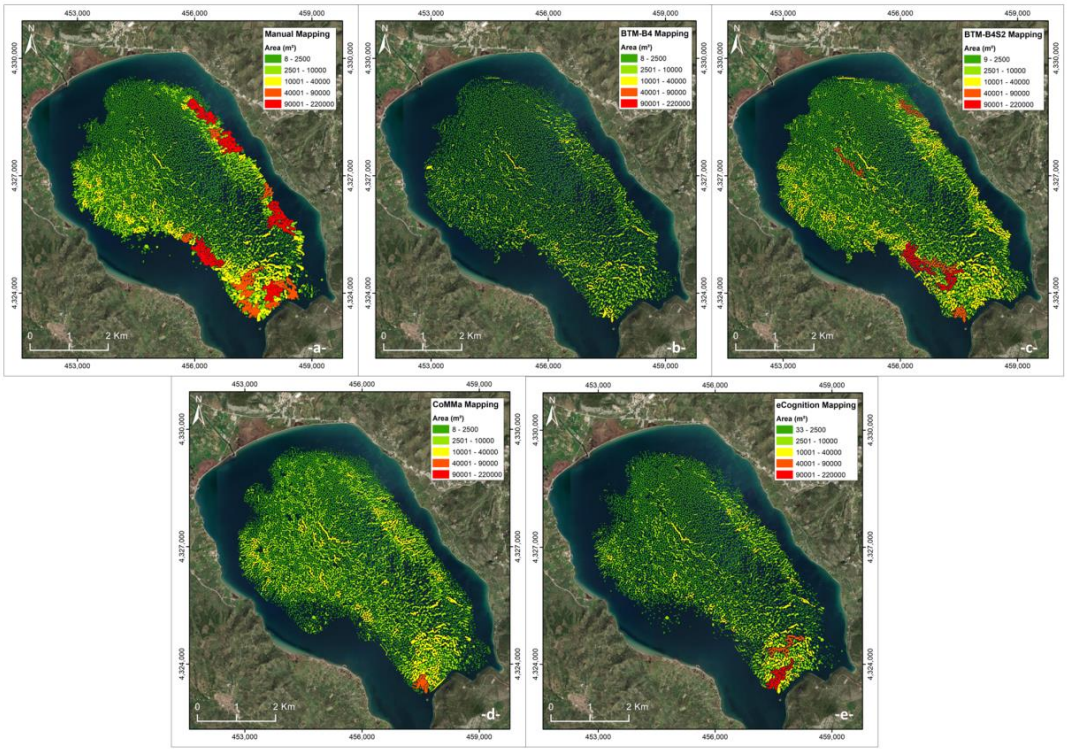


Figure 8. Categorization of the reef area, created by (**a**) manual, (**b**) BTM-B4, (**c**) BTM-B4S2 mapping, (**d**) CoMMa mapping, and (**e**) eCognition mapping.

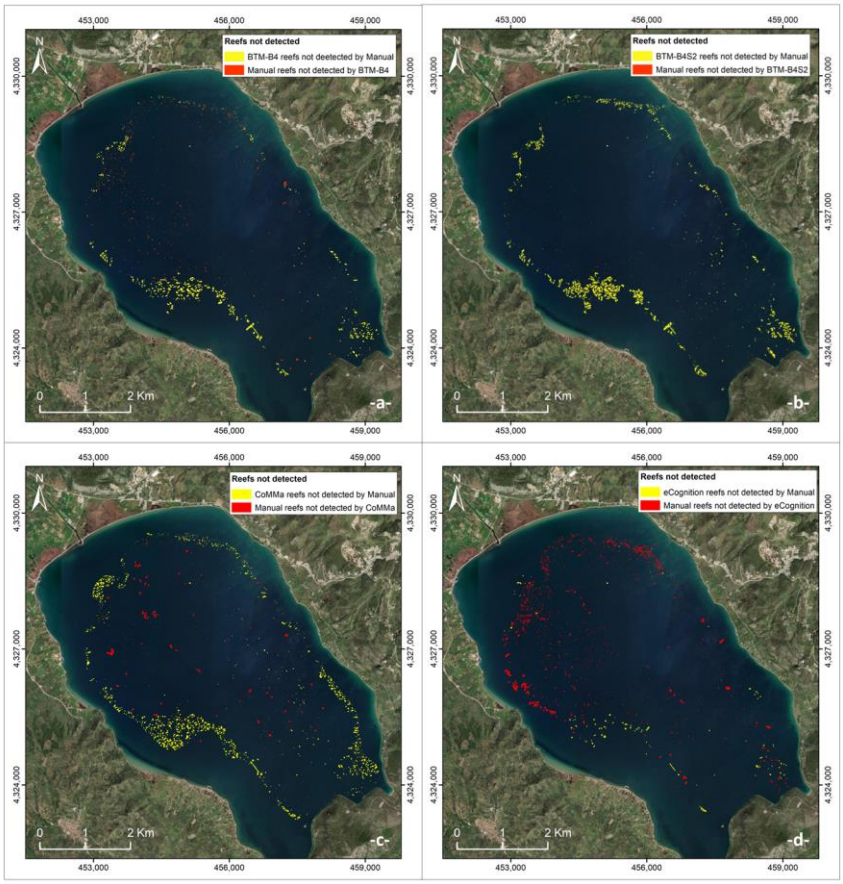


Figure 9. Map of the reefs not detected using (**a**) manual BTM-B4 mapping, (**b**) using manual or BTM-B4S2 mapping, (**c**) using manual or CoMMa mapping, and (**d**) using manual or eCognition mapping.

Table 3. Results of the geomorphometry comparison between the methods used.

	Manual vs. BTM-B4	BTM-B4 vs. Manual	Manual vs. BTM-B4S2	BTM-B4S2 vs. Manual	Manual vs. CoMMa	CoMMa vs. Manual	Manual vs. eCognition	eCognition vs. Manual
Reef Number	993	567	236	1939	477	1498	1646	97
Min. Area (m^2)	8.5	9. 7	8.5	9.3	8.5	8	8.5	83.1
Max. Area (m^2)	2112	9012	549	24,385	4604	7180	7152	4800
Mean Area (m^2)	115	534	47	276	232	301	240	641
Min. Height (m)	0.05	0.05	0.05	0.05	0.05	0.05	0.05	0.07
Max. Height (m)	0.8	1.3	0.8	1.7	1.2	2.4	2.5	1.6
Mean Height (m)	0.18	0.18	0.1	0.16	0.22	0.19	0.24	0.31

Regarding the detection accuracy (Table 4), using the Precision, Recall, and F1 Score (the accuracy of mapping), BTM-B4 resulted in the highest F1 Score value. BTM-B4S2 resulted in the highest Recall value and eCognition resulted in the highest Precision value. These calculations suggest that the eCognition results are quite precise, with the most accurate being the BTM-B4 results.

Table 4. Results of the Precision, Recall and F1 Score indexes for all the semi-automated methods.

Method	Precision	Recall	F1 Score
BTM-B4	0.92	0.97	0.94
BTM-B4S2	0.78	0.98	0.87
CoMMa	0.80	0.87	0.84
eCognition	0.98	0.78	0.87

The difference in the F1 Score results from the bigger number of reefs detected using most semi-automated methods compared with the number of reefs detected manually. The reefs not detected using manual mapping but only using BTM-B4, BTM-B4S2, CoMMa, and eCognition (Figure 9) are, as indicated by their mean values, of a small area and height. Of course, there are some exceptions, especially using the semi-automated methods. These reefs are concentrated at the shallower part of the study area (around the perimeter of the gulf) and especially near the channel connecting the gulf with the open sea, where the topography becomes more complex. The total area of reefs detected using manual mapping was also detected using CoMMa and BTM-B4S2 mapping. Observing the resulting semi-automated reefs, they exhibit a fairly realistic pattern of shape, structure, and distribution, consistent with the patterns of reef development in this area of the gulf. It is therefore possible that the semi-automated methods were able to identify some reefs that the user failed to map due to the complexity of the topography.

As for the reefs detected using both manual and semi-automated methods, a GOF index was calculated and mapcurves of the GOF values were plotted for all the methods (Figure 10). From the level of similarity between the methods, the best degree of fit resulted when the manual method was used as the RF producing a GOF of 0.53 with BTM-B4, 0.68 with BTM-B4S2, 0.56 with CoMMa, and 0.55 with eCognition. This shows that the overlap was more than 50% for the polygons, and the BTM-B4S2 polygons overlapped better than with the manual method. The extremely low GOF values reduced the unique GOF value to some extent. These low GOF values were either due to the reefs not being detected using the semi-automated methods with minimal overlap with the adjacent detected reefs, or due to artifacts in the bathymetry where the survey swaths overlap, an example of this issue is clearly identified in Figure 6iii. The reefs delimited using the semi-automated methods that exhibited this issue in the overlap areas are problematic not only in their GOF values, but also in their geomorphological characteristics, since they are perceived by ArcGIS as one reef instead of several individuals.

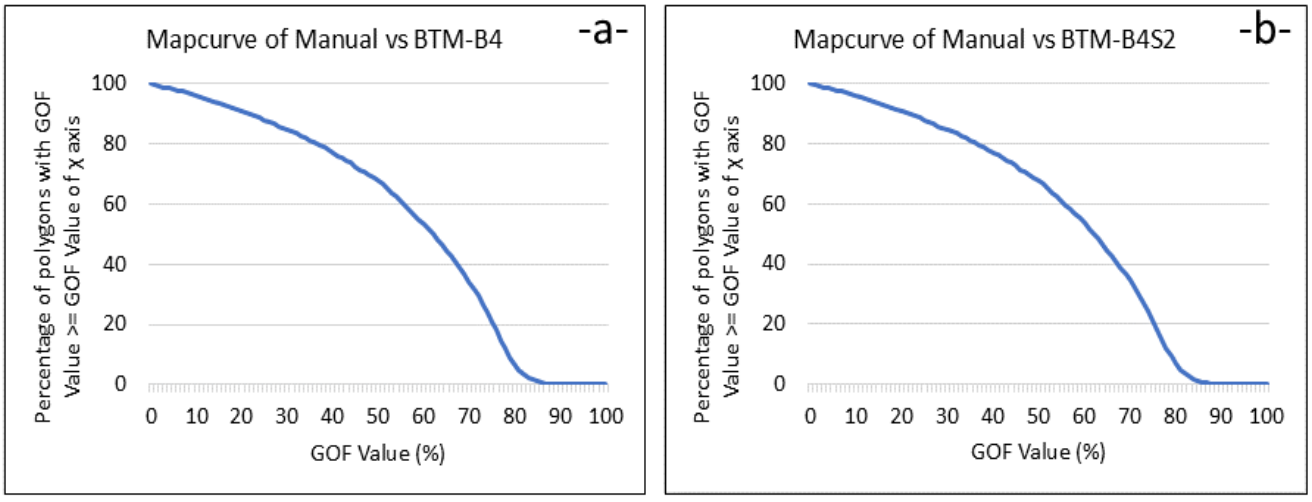


Figure 10. *Cont.*

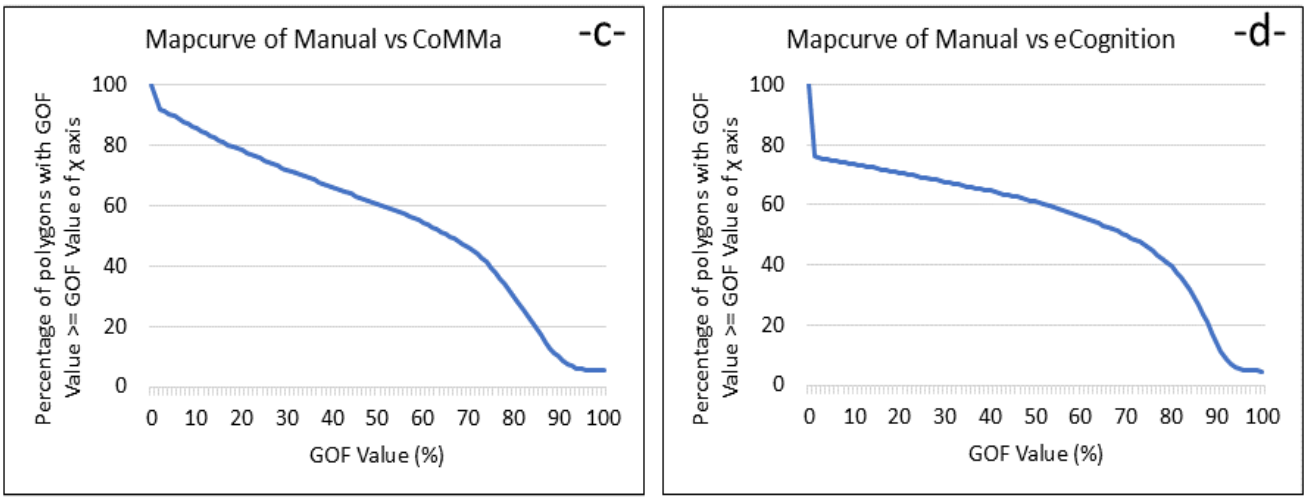


Figure 10. Mapcurve for GOF calculations using (**a**) manual as RF compared with BTM-B4, (**b**) manual as RF compared with BTM-B4S2, (**c**) manual as RF compared with CoMMa, and (**d**) manual as RF compared with eCognition.

4. Discussion

4.1. Method Comparison

Manual and semi-automated methods (BTM, CoMMa, eCognition) were utilized for the detailed mapping of the Gera Gulf reefs, using a 1 × 1 m bathymetric grid and raw backscatter data. The slope, curvature, and raw backscatter were used, while in areas of complex morphology, bathymetric profiles helped to identify the reef boundaries. Manual mapping is a time-consuming method, subject to the experience of the user. On the other hand, semi-automated methods are time-efficient, and not subject to the user, making it harder to "miss a spot". For this study, manual mapping took about 400 h of work, while semi-automated mapping, not accounting for the time initially needed for studying the basic principles and learning/understanding how to use these tools, took about 80–100 h, maybe less. For the semi-automated tools, the majority of the time was spent testing which derivatives, neighborhood sizes, etc. fitted best to the study area, excluding the case of the BTM enhancement which took more time to figure out and complete. Therefore, there is clearly a huge increase in the human effort required for manual mapping, which does not necessarily secure accurate results.

In this study, BTM initially did not seem to work properly due to the small scale of the reefs. However, by modifying the bathymetry and the slope to increase the height difference between the reefs and the seabed, the reefs became detectable by the BTM. Depending on the morphology of the seabed, it is possible that different modifications of the bathymetry and the slope may help to achieve more satisfactory results. This can be also tested/applied in other peculiar relief seafloor environments, i.e., densely distributed pockmark areas, or zones of outcropping rocks etc.

Furthermore, it is important to note that artifacts in the bathymetry affect the accuracy of the polygons (shape, detectability) detected by the semi-automated methods. It is possible to remove most of these errors using manual correction, but this can be time-consuming. Where the multibeam data are noisy with irreconcilable artifacts, manual mapping may be advised.

In any case, either by modification of the initial bathymetry or by subsequent correction of the polygon, we can obtain much more reliable and accurate results. Depending on the accuracy requirements of the research question, one method may be chosen over the other. In all cases, however, the semi-automated methods gave precise results.

In some cases of highly complex micro-relief, the semi-automated methods may work even better by identifying the morphological anomalies that the user may miss. Enhancing the data appeared to produce the best results overall. CoMMa managed to detect the same

total reef area as detected using manual mapping and although it did not result in the best results overall regarding the statistical indexes used, its results were of high accuracy, making it the most user-friendly, and time- and effort-efficient of the three tools used. An attempt was made to test what results the CoMMa tool could give using the "enhanced" rasters but this was not successful, suggesting that if this is resolved, and considering that in CoMMa there are more options for LTP derivatives, there would probably be more possibilities for testing and finding even "better-fitting" delineation results.

The fragmentation of the reefs in most semi-automated methods also plays an important role, leading to a partial distortion of the true value of the index (tending to reduce the F1 Score). It is, of course, important to note that even in manual mapping it is very likely that errors are still present. Some reefs not found using the semi-automated methods may indeed not be present but this may be only due to human error. It is possible that, in some cases, the results of the semi-automated mapping are more valid than those of manual mapping. However, the most valid and proven methodology available to date is manual mapping and this is considered to be the basis of any comparison in order to determine the accuracy of the "more modern" semi-automated seabed mapping techniques.

Most of the studies that applied BTM use it to extract the bathymetric parameters (BPI, slope, curvature, etc). The only studies that have compared manual mapping and BTM for feature delineation are Jarna et al. (2019) [32] and Menandro et al. (2020) [11]. The authors applied their methodology to cold-water coral carbonate mounds. They detected about 3500 mounds over 6.01 km^2 with manual mapping and over 7.35 km^2 with BTM mapping, distributed along an extensive study area of 76 km^2. Also, Menandro et al. (2020) [11] detected reefs with a total area of 2.96 km^2 with manual mapping and 6.85 km^2 with BTM mapping in an area of 20 km^2. In this study, the surveyed area was about 30 km^2 and more than 7000 reefs were detected on the seafloor, covering an area of 10.4 km^2 as found using the manual mapping. Even if BTM was initially unsuccessfully applied in feature detection, the modified bathymetry assisted in the detection of the reefs with a high accuracy. It can therefore be understood that the density and number of reefs in the Gera Gulf provide a real 'crash test' site for testing/comparing other semi-automated and automated feature extraction methods.

4.2. Reef Geomorphometry

Our results are consistent with those of the previous study in the area by Manoutsoglou et al. (2018) [28], but this time covering with detailed data the majority of the gulf where reefs occur. The spatial distribution of the reef height and size in the Gera Gulf was confirmed, adding more information about the geomorphometric characteristics of the reefs. In the current study, new higher-accuracy MBES data were used, thus providing a higher mapping quality for the results. Concerning the potential relationships between the geomorphometric characteristics of the reefs, the statistical testing showed that there was no significant correlation between the geomorphometric parameters. However, the only correlation identified was between the maximum slope and the height, with standard deviation $R^2 = 0.61$ for the manual, $R^2 = 0.61$ for BTM-B4, $R^2 = 0.68$ for BTM-B4S2, $R^2 = 0.70$ for CoMMa, and $R^2 = 0.55$ for eCognition (the p-value for all of these was <0.01). The lack of a strong correlation between the morphological characteristics of the reefs and the depth was again confirmed, and further, it was indicated that high slopes are mainly observed in reefs with a big relief, meaning that "tall" reefs tend to have steeper slopes rather than gentle slopes, suggesting stronger, as opposed to lateral, reef growth. Further study of their geomorphometry could help us to understand the formation and growth mechanisms that govern these peculiar formations.

5. Conclusions

In this study, high-quality MBES bathymetric and raw backscatter data were used to map manually and using three semi-automated tools the reefs of a unique and morphologically complex area that provides an ideal "crash test" site to test the feature detection

capabilities of semi-automated methods. Over 7000 reefs were distinguished and their geomorphometric characteristics were extracted. For one of the tools, bathymetric enhancement was needed in order to detect the relief of the reefs. The semi-automated methods mapped the reefs better than the manual method in areas where the terrain was really complex. Areas of noisy overlapping bathymetric data produced artifacts in the semi-automated tools. The time required to clean up these artifacts was easily compensated for by the extremely time-consuming manual mapping. It became apparent that, although with some caution, the semi-automated methods can, either independently or with slight bathymetric data modifications, produce reliable morphological and morphometric results in highly complicated submarine terrains, also contributing to benthic habitat and sensitive ecosystems mapping.

Supplementary Materials: The following supporting information can be downloaded at: https://www.mdpi.com/article/10.3390/rs16214093/s1, Supplementary Materials: GOF_script.

Author Contributions: Conceptualization, T.H. and V.L.; methodology, V.L., P.K. and R.A.; writing—original draft preparation, all authors; writing—review and editing, V.L., T.H., R.A. and A.J.W.; supervision, T.H. and A.J.W.; project administration, T.H.; funding acquisition, R.A. and A.J.W. All authors have read and agreed to the published version of the manuscript.

Funding: Riccardo Arosio was funded by the Marine Institute Grant-Aid Agreement No. PDOC/19/08/03, under the Marine Research Programme by the Government of Ireland.

Data Availability Statement: The original contributions presented in the study are included in the article/Supplementary Material, further inquiries can be directed to the corresponding author.

Acknowledgments: The authors acknowledge the valuable assistance of Ivan Theofilos Petsimeris, Anastasios Poulos, and Olympos Andreadis during the field work.

Conflicts of Interest: The authors declare no conflicts of interest.

References

1. Dolan, M.; Thorsnes, T.; Leth, J.; Al-Hamdani, Z.; Guinan, J.; Van Lancker, V. Terrain Characterization from Bathymetry Data at Various Resolutions in European Waters—Experiences and Recommendations. *Norges Geologiske Undersøkelse (Geological Survey of Norway)* 2012. Report No. 2012.045. Available online: https://www.ngu.no/upload/Publikasjoner/Rapporter/2012/2012_045.pdf (accessed on 17 October 2023).
2. Harris, T.; Baker, K. Why map benthic habitats? In *Seafloor Geomorphology as Benthic Habitat*; Elsevier: Amsterdam, The Netherlands, 2012; pp. 3–22. ISBN 9780123851406. [CrossRef]
3. Smith, M.J. Digital Mapping: Visualisation, Interpretation and Qualintification of Landforms. In *Developments in Eart Surface Processes*; Elsevier: Amsterdam, The Netherlands, 2011; Volume 15, pp. 225–251. [CrossRef]
4. Bishop, M.; James, A.; Shroder, J.; Walsh, S. Geospatial technologies and digital geomorphological mapping: Concepts, issues and research. *Geomorphology* **2012**, *137*, 5–26. [CrossRef]
5. Montereale-Gavazzi, G.; Madricardo, F.; Janowski, L.; Kruss, A.; Blondel, P.; Sigovini, M.; Foglini, F. Evaluation of seabed mapping methods for fine-scale classification of extremely shallow benthic habitats—Application to the Venice Lagoon, Italy. *Estuar. Coast. Shelf Sci.* **2016**, *170*, 45–60. [CrossRef]
6. Wright, D.J.; Lundblad, E.R.; Larkin, E.M.; Rinehart, R.W.; Murphy, J.; Cary-Kothera, L.; Draganov, K. *ArcGIS Benthic Terrain Modeler*; Davey Jones Locker Seafloor Mapping/Marine GIS Laboratory and NOAA Coastal Services Center, Oregon State University: Corvallis, OR, USA, 2005.
7. Lundblad, E.; Wright, D.; Miller, J.; Larkin, E.; Rinehart, R.; Naar, D.; Donahue, B.; Anderson, S.; Battista, T. A Benthic Terrain Classification Scheme for American Samoa. *Mar. Geod.* **2006**, *29*, 89–111. [CrossRef]
8. Guisan, A.; Weiss, S.B.; Weiss, A.D. GLM versus CCA spatial modeling of plant species distribution. *Plant Ecol.* **1999**, *143*, 107–122. [CrossRef]
9. Weiss, A.D. Topographic Positions and Landforms Analysis (Conference Poster). In Proceedings of the 21st Annual ESRI User Conference, San Diego, CA, USA, 9–13 July 2001.
10. Bridges, A.; Barnes, D.; Bell, J.; Ross, R.; Voges, L.; Howell, K. Filling the data gaps: Transferring models from data-rich to data-poor deep-sea areas to support spatial management. *J. Environ. Manag.* **2023**, *345*, 118325. [CrossRef] [PubMed]
11. Menandro, P.; Bastos, A.; Boni, G.; Ferreira, L.; Vieira, F.; Lavagnino, A.C.; Moura, R.; Diesing, M. Reef Mapping Using Different Seabed Automatic Classification Tools. *Geosciences* **2020**, *10*, 72. [CrossRef]
12. Oliveira, N.; Bastos, A.; Quaresma, V.; Vieira, F. The use of Benthic Terrain Modeler (BTM) in the characterization of continental shelf habitats. *Geo-Mar. Lett.* **2020**, *40*, 1087–1097. [CrossRef]

13. Janowski, L.; Wroblewski, R.; Dworniczak, J.; Kolakowski, M.; Rogowska, K.; Wojcik, M.; Gajewski, J. Offshore benthic habitat mapping based on object-based image analysis and geomorphometric approach. A case study from the Slupsk Bank, Southern Baltic Sea. *Sci. Total Environ.* **2021**, *801*, 149712. [CrossRef]
14. Fan, M.; Shi, S.; Ma, Y.; Wang, H.; Zhai, J.; Zhang, X.; Ning, P. High resolution geomorphological classification of benthic structure on the Western Pacific Seamount. *Front. Mar. Sci.* **2022**, *9*, 1007032. [CrossRef]
15. Gougeon, S.; Kemp, K.; Blicher, M.; Yesson, C. Mapping and classifying the seabed of the West Greenland continental shelf. *Estuar. Coast. Shelf Sci.* **2017**, *187*, 231–240. [CrossRef]
16. Pandolpho, B.T.; Urlaub, M.; Berndt, C.; Bialas, J. Identification and differentiation of vertical movement through morphological changes and stratigraphic imprint: Two distinct uplifting mechanisms in the upper Calabrian accretionary wedge, western Ionian Sea. *Basin Res.* **2023**, *36*, e12819. [CrossRef]
17. Hasan, O.; Smrkulj, N.; Miko, S.; Brunovic, D.; Ilijanic, N.; Sparica Miko, M. Integrated Reconstruction of Late Quaternary Geomorphology and Sediment Dynamics of Prokljan Lake and Krka River Estuary, Croatia. *Remote Sens.* **2023**, *15*, 2588. [CrossRef]
18. Diaz Mendoza, G.; Kramer, K.; von Ronn, G.; Schwarzer, K.; Heinrich, C.; Reimers, H.C.; Winter, C. Circular structures on the seabed: Differentiating between natural and anthropogenic origins—Examples from the Southwestern Baltic Sea. *Front. Earth Sci.* **2023**, *11*, 1170787. [CrossRef]
19. Mackin-McLaughlin, J.; Nemani, S.; Misiuk, B.; Templeton, A.; Gagnon, P.; Edinger, E.; Robert, K. Spatial distribution of benthic flora and fauna of coastal placentia bay, an ecologically and biologically significant area of the island of newfoundland, atlantic Canada. *Front. Environ. Sci.* **2022**, *10*, 999483. [CrossRef]
20. Nemani, S.; Cote, D.; Misiuk, B.; Edinger, E.; Mackin-McLaughlin, J.; Templeton, A.; Shaw, J.; Robert, K. A multi-scale feature selection approach for predicting benthic assemblages. *Estuar. Coast. Shelf Sci.* **2022**, *277*, 108053. [CrossRef]
21. Fakiris, E.; Dimas, X.; Giannakopoulos, V.; Geraga, M.; Koutsikopoulos, C.; Ferentinos, G.; Papatheodorou, G. Improved predictive modelling of Coralligenous formation in the Greek Seas incorporating large-scale, presence-absence, hydroacoustic data and oceanographic variables. *Front. Mar. Sci.* **2023**, *10*, 1117919. [CrossRef]
22. Summers, G.; Lim, A.; Wheeler, A. A Characterisation of Benthic Currents from Seabed Bathymetry: An Object-Based Image Analysis of Cold-Water Coral Mounds. *Remote Sens.* **2022**, *14*, 4731. [CrossRef]
23. Bargain, A.; Foglini, F.; Pairaud, I.; Bonaldo, D.; Carniel, S.; Angeletti, L.; Taviani, M.; Rochette, S.; Fabri, M.C. Predictive habitat modeling in two Mediterranean canyons including hydrodynamic variables. *Prog. Oceanogr.* **2018**, *169*, 151–168. [CrossRef]
24. Pearman, T.; Robert, K.; Callaway, A.; Hall, R.; Lo Iacono, C.; Huvenne, V. Improving the predictive capability of benthic species distribution models by incorporating oceanographic data—Towards holistic ecological modelling of a submarine canyon. *Prog. Oceanogr.* **2020**, *184*, 102338. [CrossRef]
25. Arosio, R.; Gafeira, J.; De Clippele, L.H.; Wheeler, A.J.; Huvenne, V.A.I.; Sacchetti, F.; Conti, L.A.; Lim, A. CoMMa: A GIS geomorphometry toolbox to map and measure confined landforms. *Geomorphology* **2024**, *458*, 109227. [CrossRef]
26. Trimble. *eCognition Developer User Guide*; Trimble Germany GmbH: Munich, Germany, 2019.
27. Ierodiaconou, D.; Schimel, A.C.G.; Kennedy, D.; Monk, J.; Gaylard, G.; Young, M.; Diesing, M.; Rattray, A. Combining pixel and object based image analysis of ultra-high resolution multibeam bathymetry and backscatter for habitat mapping in shallow marine waters. *Mar. Geophys. Res.* **2018**, *39*, 271–288. [CrossRef]
28. Manoutsoglou, E.; Hasiotis, T.; Kyriakoudi, D.; Velegrakis, A.; Lowag, J. Puzzling micro-relief (mounds) of a soft-bottomed, semi-enclosed shallow marine environment. *Geo-Mar. Lett.* **2018**, *38*, 359–370. [CrossRef]
29. Hargrove, W.; Hoffman, F.; Hessburg, P. Mapcurves: A quantitative method for comparing categorical maps. *J. Geogr. Syst.* **2006**, *8*, 187–208. [CrossRef]
30. Walbridge, S.; Slocum, N.; Pobuda, M.; Wright, D.J. Unified Geomorphological Analysis Workflows with Benthic Terrain Modeler. *Geosciences* **2018**, *8*, 94. [CrossRef]
31. Cox, E.A. A method for assigning numerical and percentage values to the degree of roundness of sand grains. *J. Paleontol.* **1927**, *1*, 179–183.
32. Jarna, A.; Baeten, N.; Elvenes, S.; Bellec, V.; Thorsnes, T.; Diesing, M. Semi-Automatic Versus Manual Mapping of Cold-Water Coral Carbonate Mounds Located Offshore Norway. *Int. J. Geo-Inf.* **2019**, *8*, 40. [CrossRef]

Disclaimer/Publisher's Note: The statements, opinions and data contained in all publications are solely those of the individual author(s) and contributor(s) and not of MDPI and/or the editor(s). MDPI and/or the editor(s) disclaim responsibility for any injury to people or property resulting from any ideas, methods, instructions or products referred to in the content.